Modeling and Simulation of the Dynamic Characteristics of Vacuum Arc in DC Interruption Based on Artificial Current Zero When the Current is Close to Zero

Jing Jiang, Lulin Kuang, Guoqing Wang, Zhongxi Liang, Yu Zhang, Le Du, Qianyi Liang, and Jinwei Lu

Abstract During the rapid current falling phase of DC breaking, due to the current drops quickly, resulting in a strong eddy current effect, which makes that the variation of the axial magnetic field (AMF) produced by AMF contact obviously lags behind that of current. Therefore, when the current approaches zero, the strength of AMF in the electrode gap is still strong. According to previous research, when the current density of high-current vacuum arc is less than 500 A/cm^2 or the strength of the AMF is greater than 10 mT/kA, the vacuum arc (VA) is a multi -cathode vacuum arc. This article aims to study the dynamic properties of VA in DC breaking process based on artificial current zero when the current approaches zero. The dynamic characteristics of single-cathode spot jet are simulated by 2D transient MHD model. The simulation results indicate that the ion density, axial current density, ion pressure, ion temperature and electron temperature of plasma decrease with the decrease of arc current, and the diffusion degree of arc shape decreases with the decrease of current.

Keywords Vacuum arc · DC interruption · Dynamic characteristics · Modeling and simulation · Transient model

1 Introduction

The flexible interconnection of large electrified wire netting based on flexible direct current transmission technology is the main construction content of China's power grid planning [1], and a high-voltage DC circuit breaker with the ability to fast isolate short-circuit faults is crucial for ensuring their safe and stable operation. Although a large number of prototypes of mechanical DC circuit breakers have been developed both domestically and internationally, there is still a significant lack of critical basic research in the rapid DC breaking process, especially the dynamic properties of VA

J. Jiang (✉) · L. Kuang · G. Wang · Z. Liang · Y. Zhang · L. Du · Q. Liang · J. Lu
CSG Guangdong Guangzhou Power Supply Bureau, Guangzhou 510000, China
e-mail: 986821689@qq.com

X. Dong and L. Cai (eds.), *The Proceedings of 2023 4th International Symposium on Insulation and Discharge Computation for Power Equipment (IDCOMPU2023)*, Lecture Notes in Electrical Engineering 1103, https://doi.org/10.1007/978-981-99-7413-9_18

in the DC breaking process, which is also one of the key factors affecting the success of DC breaking.

The DC interruption method based on forced zero crossing technique is one of the most common DC breaking technologies nowadays [2], which is very suitable for short-circuit breaking in HVDC power grids due to its characteristics.

Modeling and simulation of the arc characteristics in DC breaking process is very helpful to understand the physical characteristics of arc. Below is a brief introduction to the research process of the simulation of VA characteristics. Boxman et al. first used the theory of fluid mechanics to simulate the properties of VA in the 1970s [3]. In the 1990s, Keidar and Beilis et al. improved the numerical model of VA [4]. They coupled the electromagnetic field equation and fluid mechanics equation to solve it. Later, they considered the impacts of the azimuthal magnetic field generated by the arc and the external AMF in the simulation [5], and also solved the electron energy conservation equation to obtain the distribution of the electron temperature [6]. Schade et al. further improved the numerical model of VA by considering the energy conservation equations of electrons and ions in simulation [7, 8]. Wang et al. took into account the impacts of ion kinetic energy and viscosity in the MHD model of vacuum arc, and simulated the VA characteristics under supersonic and subsonic conditions by establishing a 2D steady-state MHD model [9, 10]. Afterwards, they extended the 2D steady-state MHD model to a 3D steady-state MHD model [11], taking into account the spatial distribution of the AMF generated by the AMF contact [12]. They also simulated and analyzed the characteristics of arc under the action of extraneous transverse magnetic field [13]. Shmelev et al. built a hybrid model, through which the VA properties in the multi-cathode spot jet mixing process were simulated [14].

At present, the research on the simulation of VA dynamic characteristics in DC breaking process is very limited. Greenwood et al. [15] built a one-dimensional model to simulate the properties of DC arc, in which fluid theory was used to simulate the characteristics of plasma. Jaidian et al. [16] established a 2D transient model on the basis of the magnetohydrodynamics theory to simulate the properties of VA during the DC breaking process. Liu et al. [17] used COMSOL software to establish a 2D fluid-chemical mixed model of DCVA on the basis of MHD theory. Hashemi et al. [18] built a 2D transient MHD model, through which the characteristics of DCVA in a rapid transverse magnetic field were simulated. Wang et al. [19] built a 3D transient MHD model to simulate the dynamic properties of VA during the rapid current falling phase in DC interruption, and also conducted simulation calculation for the initial diffusion stage of DCVA [20].

This article aims to study the dynamic properties of VA in direct current interruption on the basis of artificial current zero when the current is close to zero. A 2D transient MHD model is built, based on which the dynamic characteristics of single cathode spot jet are simulated. The dynamic characteristics of ion pressure, ion number density, axial current density, ion temperature and electron temperature of single cathode spot jet when the current is close to zero were obtained.

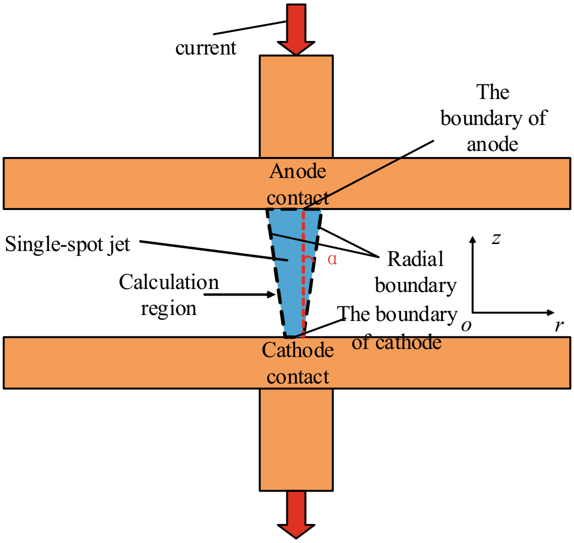

Fig. 1 Physical model of single-cathode spot jet

2 Physical Model and Assumptions

2.1 Physical Model

The simulation uses a 2D transient MHD model [21]. Figure 1 is the physical model diagram of this simulation. The simulation model contains a cathode spot jet with a diameter of 2 mm. The electrode distance is 4 mm. The calculation area of the model is a trapezoid, and the length of the bottom surface is consistent with the diameter of the cathode spot jet. The two sides are free boundaries. The cathode is at the bottom, and the anode is at the top. The initial incidence angle of the cathode jet is α, which is the angle between the side boundary and the perpendicular line of the cathode surface.

2.2 Modeling Assumptions

In the model of this article, the following assumptions were made:

(1) Assuming that the single-cathode spot jet is not affected by others;
(2) Assuming the AMF in the calculated area during the simulation process is a constant value;
(3) Assuming that the model is an axisymmetric model;
(4) The plasma in the calculated region is highly ionized, containing only ions and electrons;

(5) Assuming that the plasma in the calculated area meets the quasi-neutral condition;
(6) Assuming that the vacuum arc satisfies fluid theory to describe;
(7) Ions and electrons are regarded as ideal gas;
(8) Assuming that both ions and electrons follow the Maxwell distribution;
(9) The anode is not yet active and passively receives ions and electrons that arrive at the anode.

2.3 Boundary Conditions

The single-cathode spot jet can be regarded as a vacuum arc in which ions are in a supersonic state. For the boundary of the cathode, base on previous experimental data, the velocity of ion that near the cathode $u = 10^4$ m/s, the electron temperature $T_e = 1.5$ eV, the ion temperature $T_i = 0.3$ eV, and the average charge of ion $z_i = 1.85$. Assuming a uniform distribution of axial current density on the cathode side.

The boundary condition on the anode side of the equation of electron energy conservation is:

$$2.5 n_e k v_z T_e + q_{ez} = n_e v_z e \cdot \left(\frac{2kT_e}{e} - \varphi_{sh} \right) \quad (1)$$

n_e is the electron number density; k is the Boltzmann constant; v_z is the electron axial velocity; T_e is the electron temperature; φ_{sh} is the potential of the anode sheath.

Assuming that the electron energy conservation equation is adiabatic on the side boundary, that is:

$$\partial T_e / \partial n = 0 \quad (2)$$

The boundary condition of the magnetic transport equation on the cathode side is:

$$B_\theta = \frac{\mu_0 I(t)}{\pi R^2} \cdot \frac{x}{2} \quad (3)$$

B_θ is the azimuthal magnetic field; R is the radius of the column of arc, x is the x-axis coordinate value of the grid of the cathode side.

The boundary condition of the magnetic transport equation at the side boundary is:

$$B_\theta = \frac{\mu_0 I(t)}{2\pi r} \quad (4)$$

r is the distance between the grid of the side boundary and the axis of the arc column.

$$\frac{\partial B_{\theta}}{\partial z}=-\mu_0\sigma(-v_z B_{\theta}-\frac{1}{n_e e}j_{\theta}B_z+\frac{1}{n_e e}\frac{\partial P_e}{\partial r}+g_t\frac{k}{e}\cdot\frac{\partial T_e}{\partial r}+\frac{\partial\varphi_{sh}}{\partial r}) \tag{5}$$

j_{θ} is the azimuthal current density; B_z is the strength of the axial magnetic field; p_e is the electron pressure; g_t is the thermodynamic constant.

3 Simulation Results and Discussion

The Simulation condition is that the current of single-cathode spot jet drops from 200 to 50 A within 15 μs. The initial calculation time is 20 μs before the current crosses zero. During the rapid current falling phase, the variation of the AMF lags significantly behind that of current. Meanwhile the simulation calculation time is very short, and the simulation area is very small, so the AMF in the calculated area during the simulation process sets as a constant value of 100 mT. Due to the large current drop rate during the rapid current falling phase, the arc current can be approximately considered as a linear decrease. The simulation model is a transient model, and time step of this simulation is 0.5 μs. In this paper, the simulation results of the characteristics of single-cathode spot jet at four different time (the corresponding arc current value at four different time is 200, 150, 100 and 50 A respectively) are taken for analysis. The simulation results are as follows.

3.1 Ion Number Density

Figures 2 and 3 indicate that as the current decreases, the ion number density decreases significantly. Before the current close to zero, due to the small current carried by a single jet, the plasma in arc column is distributed in a diffuse manner. At the corresponding time of each arc current value, the ion number density decreases gradually from cathode to anode, and also decreases from the center of the arc column along the radial direction to the edge. Comparing the distribution of ion number density at the corresponding moments of different arc current values, it is found that as the current decreases, the overall ion number density decreases, and the diffusion degree of the jet gradually weakens. The reason is that the decrease of ion number density will lead to the decrease of radial pressure gradient, and then the radial diffusion velocity of plasma decreases, so the overall diffusion of the single-cathode spot jet weakens.

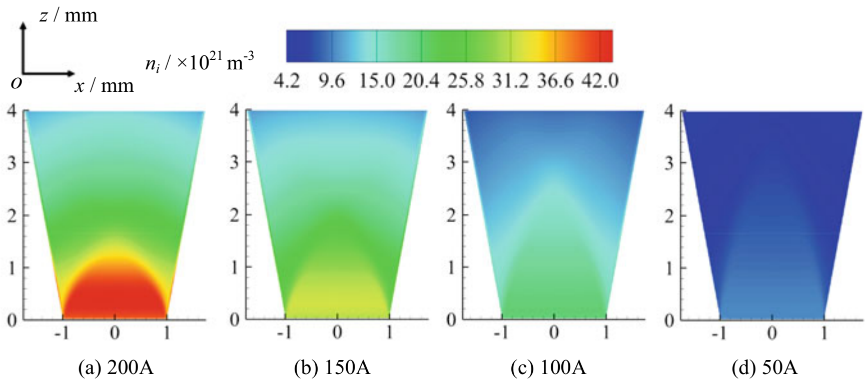

Fig. 2 Distribution of the ion number density (cathode at the bottom, anode at the top)

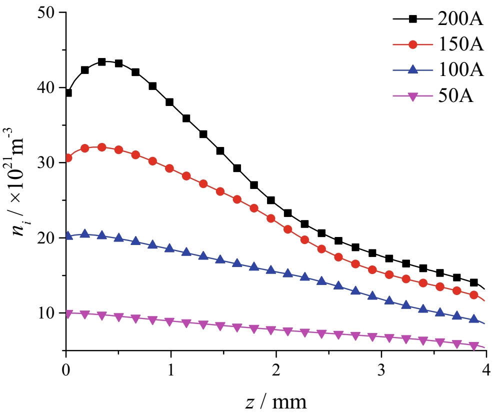

Fig. 3 Distribution of the ion number density on the arc column centre axis (cathode is at z = 0 mm, anode is at z = 4 mm)

3.2 Axial Current Density

Figures 4 and 5 show that as the current decreases, the axial current density of the jet also decreases. At the corresponding time of each arc current value, the axial current density and its gradient gradually decrease from the cathode to the anode. This is because in a low current diffusion state arc, the pinch force generated by the self-generated magnetic field on the ions is smaller than the ion pressure. So the distribution of the axial current density is consistent with the ion number density.

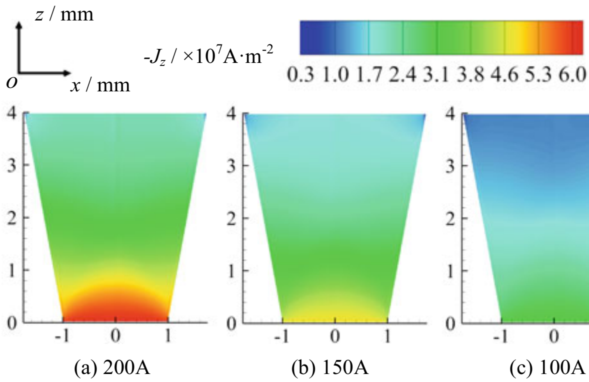

Fig. 4 Distribution of the axial current density

Fig. 5 Distribution of the axial current density on the arc column centre axis

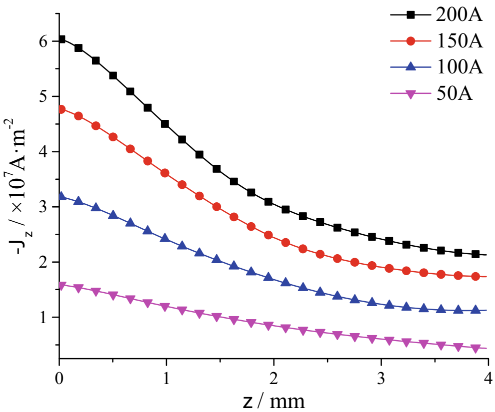

3.3 Ion Pressure

Figures 6 and 7 demonstrate that as the current decreases, the ion pressure decreases. As shown in Fig. 7, the ion pressure at the central axis increases first and then decreases. The peak value of ion pressure is not on the cathode, but above the cathode. As the current decreases, the peak position of the ion pressure is farther away from the cathode, which is quite different from the distribution of the ion number density.

3.4 Ion Temperature

Figures 8 and 9 show that as the current decreases, the ion temperature decreases. The main reasons are as follows: Firstly, with the decrease of the current, the generated

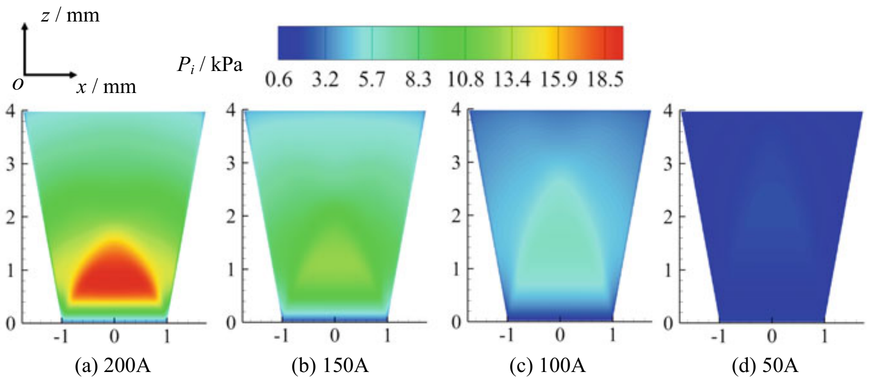

Fig. 6 Distribution of the ion pressure

Fig. 7 Distribution of the ion pressure on the arc column centre axis

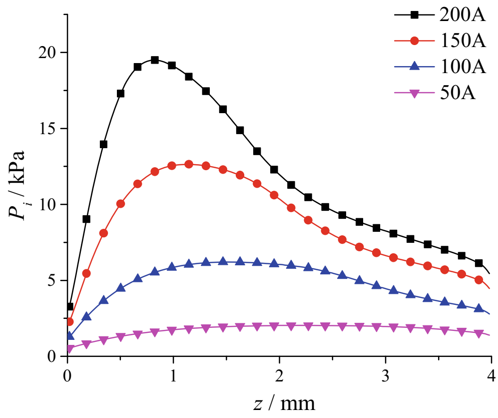

Joule heat decreases significantly, leading to the decrease of the electron temperature. The heat obtained by ions in the process of electron and ion heat exchange decreases, so the ion temperature decreases. Secondly, as the current decreases, the deceleration of ions by the radial current and the azimuthal magnetic field weakens, so the kinetic energy of the ions converted into internal energy decreases, causing the ion temperature to decrease.

3.5 Electron Temperature

Figures 10 and 11 indicate that as the current decreases, the electron temperature decreases. Compared with the ion temperature, the electron temperature is higher. The distribution of the electron temperature from cathode to anode increases first and then decreases, which is like that of the ion temperature. The reason why the

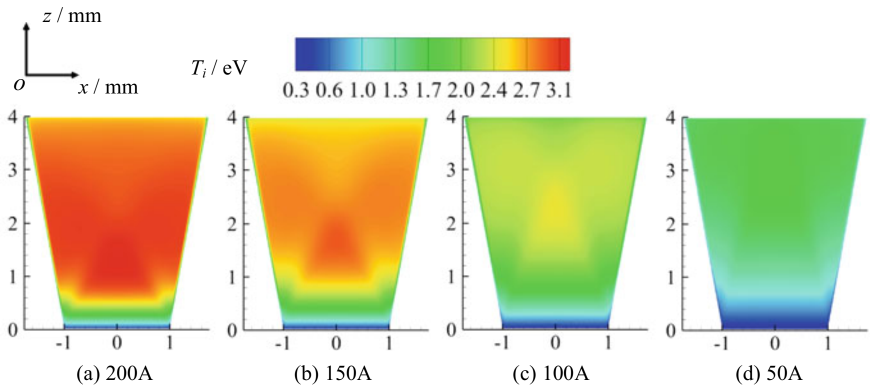

Fig. 8 Distribution of the ion temperature

Fig. 9 Distribution of the ion temperature on the arc column centre axis

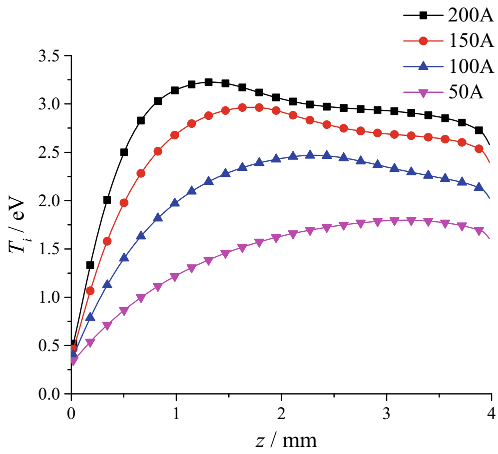

electron temperature close to the anode will decrease is that the electron consumes energy during the process of passing through the anode sheath.

4 Conclusions

This article establishes a 2D transient MHD model to simulate the dynamic properties of VA during DC breaking process based on artificial current zero when the current approaches zero. The following conclusions are obtained:

(1) The ion density, the axial current density, the ion pressure, the ion temperature and the electron temperature in the region of the arc column decrease as the arc current decreases.

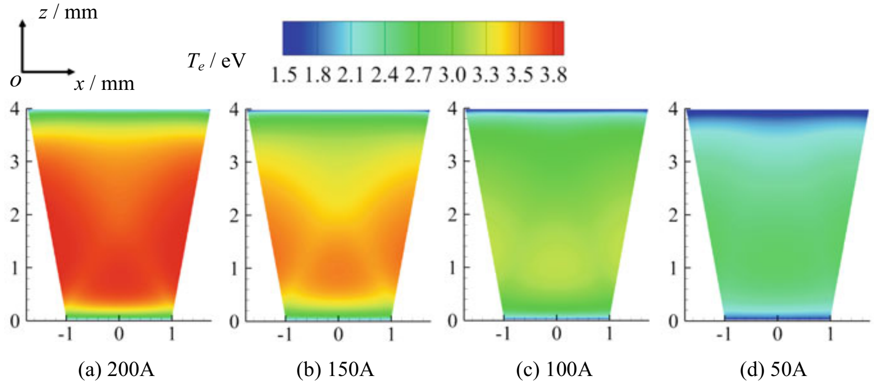

Fig. 10 Distribution of the electron temperature

Fig. 11 Distribution of the electron temperature on the arc column centre axis

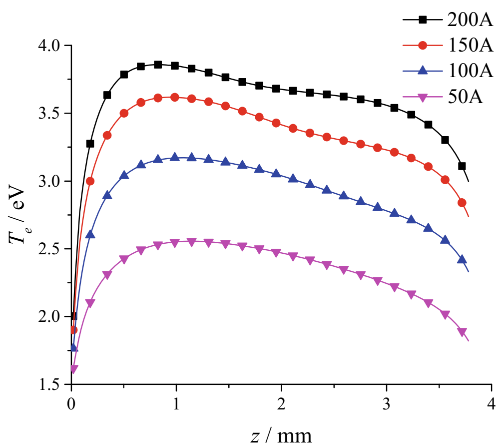

(2) As the current decreases, the diffusion degree of plasma weakens.

Acknowledgements This work was funded by the Science and Technology Program of China Southern Power Grid (Intelligent Individual Soldier Patrol and Inspection Device for the Distribution Grid, 082100KK58200002).

References

1. Tang G, Luo X, Wei X (2013) The technology of Multi-terminal HVDC transmission and DC power grid. Proc CSEE 33(10):8–17 (in Chinese)
2. Shi Z, Jia S (2015) Review of research on high-voltage DC circuit breaker. High Volt Appar 51(11):1–9 (in Chinese)

3. Boxman R (1977) Magnetic constriction effects in high-current vacuum arcs prior to the release of anode vapor. J Appl Phys 48(6):2338
4. Keidar M, Beilis I, Boxman R et al (1996) 2D expansion of the low-density interelectrode vacuum arc plasma jet in an axial magnetic field. J Phys D-Appl Phys 29(7):1973–1983
5. Beilis I, Keidar M, Boxman R et al (1998) Theoretical study of plasma expansion in a magnetic field in a disk anode vacuum arc. J Appl Phys 83(2):709
6. BeilisI, Keidar M (2002) Electron temperature in the expanding cathode plasma jet in a vacuum arc. In: 20th international symposium on discharges and electrical insulation in vacuum. IEEE, Tours, France, pp 535–538
7. SchadeE, Shmelev D, Sfv E et al (2002) Numerical modeling of plasma behavior and heat flux to contacts of vacuum arcs with and without external axial magnetic field (AMF). In: 20th international symposium on discharges and electrical insulation in vacuum, pp 44–51. IEEE, France
8. Schade E, Shmelev D (2003) Numerical simulation of high-current vacuum arcs with an external axial magnetic field. IEEE Trans Plasma Sci 31(5):890–901
9. Wang L, Jia S, Shi Z et al (2005) Simulation research of magnetic constriction effect and controlling by axial magnetic field of vacuum arc. Plasma Sci Technol 7(1):2687–2692
10. Wang L, Jia S, Shi Z et al (2006) High-current vacuum arc under axial magnetic field: numerical simulation and comparisons with experiments. J Appl Phys 100(11):113304
11. Wang L, Luo M, Deng J et al (2021) Numerical simulation of multi-species vacuum arc subjected to actual spatial magnetic fields. IEEE Trans Plasma Sci 49(11):3652–3662
12. Qian Z, Wang L, Jia S et al (2015) The 3D simulation of high-current vacuum arc under combined effect of actual magnetic field and external transverse magnetic field. IEEE Trans Plasma Sci 43(8):2275–2282
13. Qian Z, Wang L, Jia S et al (2014) 3-D simulation of plasma's rotation behavior in high current vacuum arcs under realistic spatial magnetic field profile. IEEE Trans Plasma Sci 42(10):2708–2709
14. ShmelevD, Uimanov I (2014) Hybrid computational model of diffuse high-current vacuum arc. In: 26th international symposium on discharges and electrical insulation in vacuum, pp 269–272. IEEE, Mumbai, India
15. Childs S, Greenwood A (1980) A model for DC interruption in diffuse vacuum arcs. IEEE Trans Plasma Sci 8(4):289–294
16. Jadidian J (2009) A compact design for high voltage direct current circuit breaker. IEEE Trans Plasma Sci 37(6):1084–1091
17. Liu X, Liu C, Zou J (2015) Comparative analysis of AC and DC vacuum arc plasma characteristics. J Vac Sci Technol 35(10):1203–1208 (in Chinese)
18. Hashemi E, Niayesh K (2020) DC current interruption based on vacuum arc impacted by ultra-fast transverse magnetic field. Energies 13(18):4644
19. Wang L, Zhang Z, Chen J et al (2022) 3D transient MHD simulation of DC breaking vacuum arc based on artificial current zero. J Appl Phys 132(6):063301
20. Wang L, Zhang Z, Yang Z et al (2022) 3-D dynamic simulation of the initial expansion process of vacuum arc plasma in DC interruption. IEEE Trans Plasma Sci 50(5):1301–1312
21. Zhang L, Jia S, Wang L et al (2011) Simulation of vacuum arc characteristics under four kinds of AMFs and comparison with experimental results. Plasma Sci Technol 13(4):462–469